JP2J.2 DUAL-DOPPLER ANALYSIS OF HURRICANE ISABEL AT LANDFALL: A RESEARCH EXPERIENCE FOR UNDERGRADUATES

Renee A. Curry and Michael I. Biggerstaff*
University of Oklahoma, Norman, Oklahoma

1. INTRODUCTION

Much of what is known about the structure of hurricanes, particularly the vertical motion within the storm, is from observations taken by aircraft over oceans. By necessity, these observations focused either on mesoscale characteristics that could be resolved with airborne Doppler radars (Barnes et al. 1983; Jorgensen 1984) or on statistical characteristics of convective-scale features diagnosed from in situ samples along the flight path (Jorgensen et al. 1985).

Black et al. (1994; 1996) combined these strategies in their statistical analyses of the vertical incidence data collected with the tail Doppler radar along the airplane flight track through several Atlantic hurricanes. They determined the vertical distributions of vertical drafts retrieved from the Doppler observations for different parts of hurricanes and found good agreement with earlier in situ observations at the altitudes common to both studies.

While the statistical distribution of vertical motion might be well established, with the notable exception of Barnes et al. (1991), there is a lack of detailed analyses of convective-scale circulations in hurricane rainbands that relate the spatial pattern and vertical structure of vertical motion to precipitation features. This is particularly true for observations of vertical motions during landfall when the aircraft is limited by safety concerns arising from the potential for tornadic circulations (Gentry 1983; McCaul 1987).

The scarcity of detailed airflow observations for hurricanes at landfall limits attempts to validate numerical simulations of land-falling tropical cyclones (Jones 1987). Moreover, the lack of understanding in changes to the vertical motion as the storm makes landfall contributes to errors in forecasting the amount and distribution of heavy rain and associated flooding.

* *Corresponding author:* Michael I. Biggerstaff, School of Meteorology, University of Oklahoma, Norman, OK 73019; email: drdoppler@ou.edu.

As noted by Rappaport (2000), the greatest lost of life associated with US hurricanes over the past 30 years has been from inland fresh-water flooding. Consequently, the US Weather Research Program has placed special emphasis on improving quantitative precipitation forecasts (QPFs) for land-falling hurricanes (Marks et al. 1998; Elsberry 2002).

With the advent of mobile Doppler radars (Wurman et al. 1997; Biggerstaff et al. 2005) detailed observations of the airflow across mesoscale regions of land-falling tropical cyclones can be obtained. This was best demonstrated by deployment of the two C-band Shared Mobile Atmospheric Research and Teaching (SMART) radars during the Characterization of Atmospheric Turbulence and Flood Initiation and Verification Experiment (CAT-FIVE; Biggerstaff et al. 2005) in which 13 hours of continuous mobile Doppler data were collected during the landfall of Hurricane Isabel in North Carolina, USA on 18-19 September 2003.

Here, we examine five consecutive dual-Doppler volumes collected over a 12-min period during the early stages of landfall. Several rainbands, primarily stratiform in structure, were sampled. While the resolvable updraft scale (~ 3 km) from the dual-Doppler analyses is larger than the median diameter (~2 km) of observed updraft cores (Jorgensen et al. 1985), the spatial and temporal continuity of retrieved structure provides confidence in the quality of the results.

We found several banded vertical velocity features that contained convective scale cellular structure. Some of the features were relatively shallow and were oriented roughly parallel to the coast and quasi-perpendicular to the flow. Other vertical motion bands were deep and, at mid-levels, were oriented roughly parallel to the main precipitation features. Additionally, a frontal zone in the area contributed to a low-to-midlevel region of ascent just offshore.

In general, the dual-Doppler analyses presented here illustrates the complex pattern of circulations that arise as rainbands interact with coastal topography, even relatively low

altitude topography like that found over the North Carolina coast.

2. DATA

Hurricane Isabel was a classic Cape Verde tropical cyclone that originated in an easterly wave off the western coast of Africa on 1 September 2003. Although at one time a Saffir-Simpson scale category five hurricane, Isabel made landfall as a category two storm near Drum Inlet on the Outer Banks of North Carolina on 18 September 2003 (Beven and Cobb 2004).

The data used in this project were taken from the two SMART-radars deployed along a 54 km north-south oriented baseline with SMART-R1 (SR-1) stationed at Washington, North Carolina, and SMART-2 (SR-2) located at New Bern, North Carolina (Fig. 1). Both deployment sites were municipal airports. While providing a logistically convenient location with adequate evacuation facilities, the airports were surrounded by tall trees that blocked the lowest 1-degree of the radar horizon.

The dual-Doppler lobes (Fig. 1) are located to the east and west of the radar baseline and represent the region in which the three-dimensional component of the wind may be retrieved. Coordinated data collection between the two SMART-Rs began around 0930 UTC and ended around 2200 UTC on 18 September 2003, yielding observations of numerous rainbands and the eyewall as Hurricane Isabel made landfall (Fig. 1).

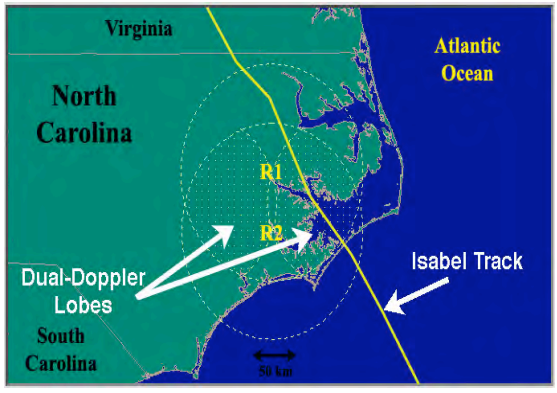

Fig. 1. Track of Hurricane Isabel relative to dual-Doppler lobes from the SMART radars. The dashed circular rings indicate the operational radar range. The stippled region is the area available for dual-Doppler analysis. SR-1 (R1) is located to the north, and SR-2 (R2) is located to the south. The yellow line is the path of the eye of Hurricane Isabel. Note that the hurricane tracked directly through the eastern lobe of the dual-Doppler coverage area.

The objectives of CAT-FIVE included both precipitation mechanisms and boundary-layer turbulence characteristics. The radars repeated a pre-determined sequence of scans on a 40-minute cycle with two 20-minute blocks of time. The first 20 minute-block was dedicated to precipitation studies and the second block to turbulence. This study makes use of the precipitation mode that contains both full 360º volume scans and 130° azimuthal sector scans over one of the dual-Doppler lobes (Table 1).

Table 1. Elevation angles used by the SMART radars during Hurricane Isabel. Parenthesis ( ) indicate elevation angle of SR-2, if different from SR-1. SR-2 did not collect the 32.7° tilt during the 130° sector scan.

130° Sector scan	360° Volume scan
1.0 (0.8)	1.0 (0.8)
1.5	1.5
2.3	2.3
3.2	3.2
4.3	4.3
5.4	5.4
6.9	6.8
8.7	8.4
10.8	10.2
13.2	12.2
15.9	14.5
18.9	17.1
22.2	20.2
25.7	23.2
29.2	26.9
32.7	30.5
	34.6

The 130º sector scans required two minutes to complete while the full 360º volume scan required four and a half minutes. Here, we examine results from the period 1044 – 1056 UTC that contain four of the 130° sector scans and one of the full 360° sector scans (Table 2). As the hurricane center was located well offshore at this time (~250 km), only data from the eastern dual-Doppler lobe was used.

Table 2. Starting times and types of the volume scans analyzed in this study..

Time (UTC)
10:44:30 (east sector)
10:47:00 (east sector)
10:49:30 (east sector)
10:52:00 (full)
10:56:30 (east sector)

3. METHODS

The 100 km operational range of the SMART radars during Isabel provided a Nyquist velocity of ± 18.75 m s^{-1}. Doppler data were edited and dealiased using SOLOii (Oye et al. 1995). At low tilts, some of the radar beams experienced blockage by trees and redirection by nearby metallic buildings. Rays that appeared randomly redirected were deleted from the dataset.

The edited data were interpolated to Cartesian coordinates using REORDER (Oye et al. 1995) with a Cressman weighting interpolation method that employed a beamwidth-dependent radius of influence. The radius of influence varied with range such that high resolution in the region closest to the radar was retained while farther from the radar low resolution occurred. This is consistent with the inherent resolution associated with finite beamwidth radar. The dimensions of the analysis grid extend from 0 to 100 km in the x (east-west) direction, from -40 to 94 km in the y (north-south) direction, and from 0 to 13 km in the z (vertical) direction with SR-2 being the origin of the coordinate system. The horizontal spacing between points is 1 km and the vertical spacing is 0.5 km.

REORDER output from the two radars were combined and wind fields were retrieved using CEDRIC (Custom Editing and Display of Reduced Information in Cartesian Space; Mohr et al. 1986). Our analysis takes into account the radar reflectivity-based estimated fall speed of the participation particles following the procedure outlined in Biggerstaff and Houze (1991). Individual grid points were vertically aligned using an advection speed of 35 m s^{-1} from 75 degrees. A two-step Leise (1981) filter was applied to the horizontal wind components before computing divergence. This led to a resolvable horizontal wavelength scale of around 6 km. The resolvable vertical scale, determined by the elevation tilts of the volume scans, was ~2-4 km wavelength depending on the range from the radar.

The divergence field was integrated downward using a fraction of the integrand as a boundary condition to retrieve vertical motion. The horizontal winds were corrected for the vertical motion, and the flow field recomputed iteratively until the solution of the winds converged. Only 2-3 iterations were necessary for the solution to converge.

4. RESULTS

4.1 *Interaction With Land*

North Carolina has a complex coastal land form (Fig. 2). The northern part of the eastern dual-Doppler lobe is characterized by low-lying forested marsh with numerous salt-water inlets and lakes. The central part of the analysis domain has relatively open water in the eastern half (Pamlico Sound) and land divided by major two inlets in the western half. The two Doppler radars were deployed at the western end of the inlets. The southern part of the domain is similar in character to the central region but the land mass extends farther eastward, forming a small peninsula. The complex distribution of land appeared to affect the flow in three ways.

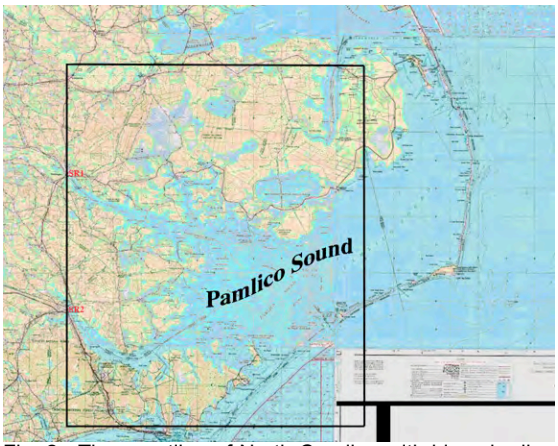

Fig. 2. The coastline of North Carolina with blue shading representing water and yellow shading indicating land. The box marks the analysis domain associated with the eastern dual-Doppler lobe. Radar locations are labeled in red.

On the mesoscale, there was a distinct two-branch flow with easterly winds in the northern half of the domain across the land mass and northeasterly flow in the southern part of the domain over the open water and across that part of the coast (Fig. 3). While this two-branch circulation appears to have been influenced by the coastal interaction, it is important to note that this flow structure was evident throughout the depth of the analysis.

Besides the difference in the northerly wind component, there was a also distinct difference in the area-averaged vertical motion across the two flow regimes. The easterly flow was dominated by mean subsidence and the northeasterly flow was dominated by mean ascent (Fig. 4). This distinction was evident from 3.5 km altitude and above. Below 3.5 km, both regions appeared to be associated with mean descent. The melting level for this part of the storm system was around 5.5 km altitude. Hence, the mesoscale updraft

extended below the melting level at this time. Later, we will show that flow over a frontal zone contributed to the upward motion at lower levels.

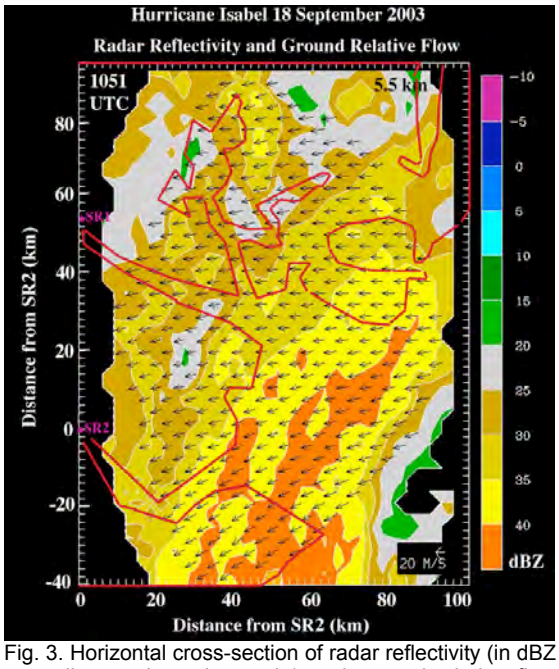

Fig. 3. Horizontal cross-section of radar reflectivity (in dBZ according to the color scale) and ground-relative flow (reference vector in lower right corner of plot) at 5.5 km and 1051 UTC showing the two-branch flow. The red overlay approximately separates land from water. The analysis domain is oriented such that the X-axis points towards the east.

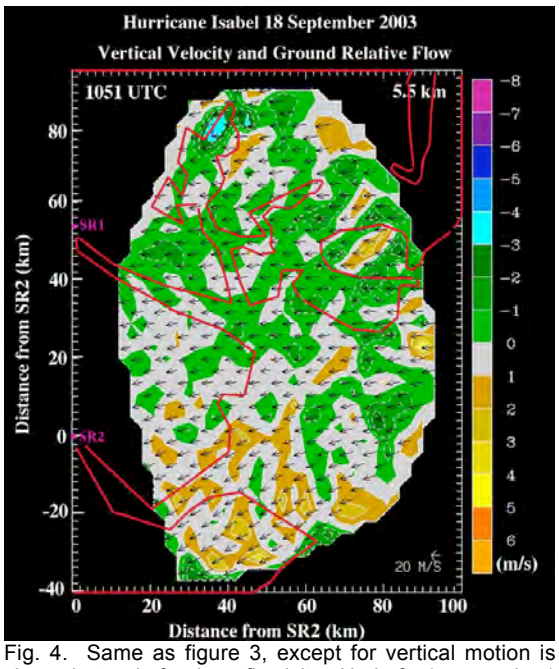

Fig. 4. Same as figure 3, except for vertical motion is shown instead of radar reflectivity. Updrafts (warm colors) and downdrafts (cold colors) are as indicated by the color scale.

Multiple curving precipitation bands extended across Pamlico Sound and aligned with the northeasterly flow. These bands were just starting to propagate across the main shore of North Carolina. The northeasterly flowing branch of the rain band circulation, with its deep mesoscale ascent, was associated with the highest radar reflectivity part of the rain bands. The easterly flow regime, with mean subsidence, was associated with significantly lower radar reflectivity.

On a convective scale, the interaction between the airflow and coastal terrain produced small-scale perturbations in vertical motion with magnitudes reaching a few meters per second. This is particularly true in the southern part of the analysis domain where the flow was perpendicular to the peninsula at the south end of Pamlico Sound (Fig. 5).

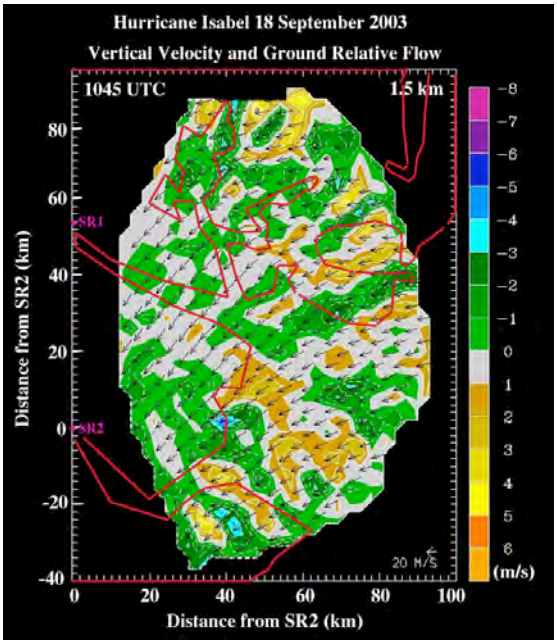

Fig. 5. Horizontal cross-section of vertical velocity (in m s^{-1} according to the color scale) and ground-relative flow (reference vector in lower right corner of plot) at 1.5 km and 1045 UTC showing the convective perturbations produced by flow over the land. The red overlay approximately separates land from water. The analysis domain is oriented such that the X-axis points towards the east.

Vertical cross-sections (not shown) of these convective drafts indicate that they are mostly confined to the lowest 5 km of the troposphere. It is likely that their true depth was less as the vertical resolvable scale in that part of the analysis domain is ~4 km due to the distance from SR1.

A vertical cross-section taken through the central part of the analysis domain (at Y=11 km), where the vertical resolution is better, illustrates the third impact of the airflow's interaction with land, namely the deceleration in the across-shore component of the wind (Fig. 6). The east-west wind component decreases from >30 m s^{-1} at X= 40 km to <20 m s^{-1} at X= 15 km. In contrast, the northerly wind component increased over that region, particularly right at the shoreline (X=40 km). The change in speed and direction was most evident in the lowest 3 km of the atmosphere and occurred at this geographic location in all five analyses. The stationary nature of this transition contrasts with advection of radar reflectivity and the overall airflow pattern, suggesting that the transition is tied to the topography.

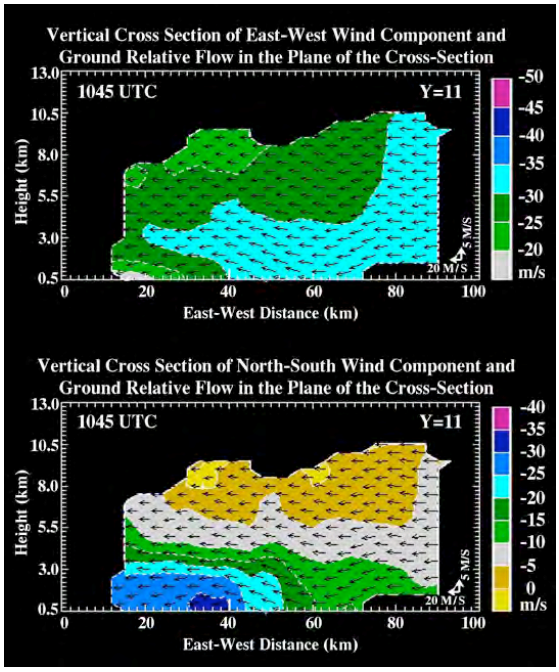

Fig. 6. Vertical cross sections of east-west wind (top panel) and north-south wind (bottom panel) taken at Y=11 km from the 1045 UTC analysis. Wind speeds are in m s^{-1}, according to the color scale. Arrows represent ground relative flow in the plane of the cross-section (U and W). The shoreline is located at X=40 km.

The decrease in across-shore flow was associated with a broad region of convergence at low levels. While the vertical velocity field had many convective scale perturbations associated with it, there was a shallow north-south oriented rain band farther inland that may have been aided by the broad region of low-level convergence across the main part of the coast (Fig. 7).

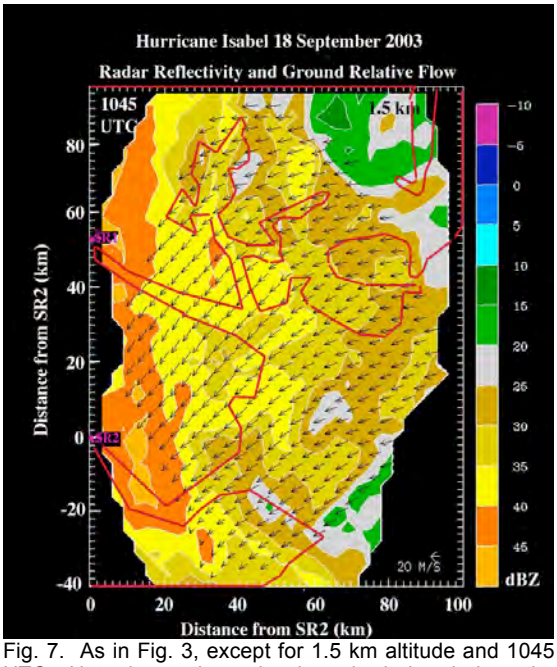

Fig. 7. As in Fig. 3, except for 1.5 km altitude and 1045 UTC. Note the north-south oriented rain band along the western edge of the domain.

4.2 Interaction With Frontal Zone

The structure of the north-south wind component in Fig. 6 suggests that there was another transition in the flow offshore. The northerly component started increasing at X=60 km. Indeed, the peak radar reflectivity associated with the radar bright band and indicative of the 0° isotherm (Bemis 1950) sloped downward rather sharply from 5 km altitude at X=60 km to under 3 km altitude at X=40 km (Fig. 8). A broad-scale updraft with speed of 2-4 m s^{-1} was found in the lowest 3 km.

A sloping 0°C isotherm, region of moderately strong broad-scale ascent, and increase in the northerly component of wind towards the cold air are all features typically associated with a frontal zone. A front did pass through North Carolina prior to Isabel's landfall. Apparently the frontal zone was located just offshore at this time and contributed to a broad region of upward motion at low levels despite being underneath a stratiform hurricane rain band where one might expect to find a region of mesoscale descent (Marks and Houze 1987).

The impact that the frontal circulation had on the heavy rain and flooding associated with Isabel's landfall is unclear. It is likely that the low-level flow ascending the frontal surface had already been heavily modified by the rain bands farther to the east, where

strong subsidence was found from mid-to-low levels.

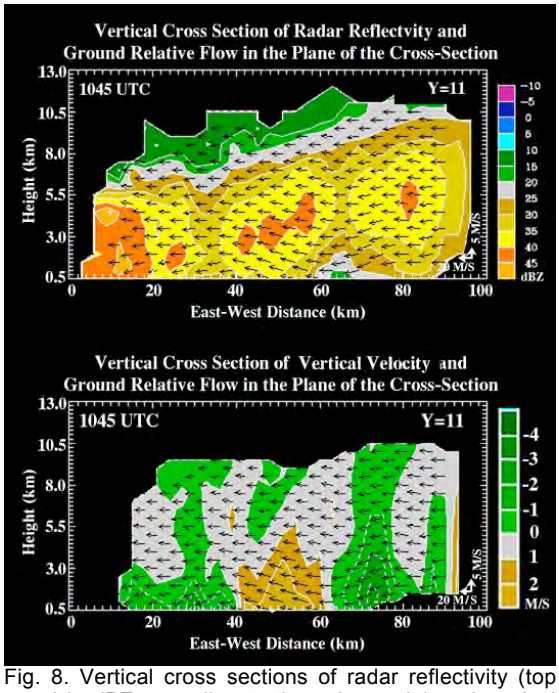

Fig. 8. Vertical cross sections of radar reflectivity (top panel in dBZ according to the color scale) and vertical velocity (bottom panel, in m s^{-1} according to the color scale) taken at Y=11 km from the 1045 UTC analysis.. Arrows represent ground relative flow (U and W) in the plane of the cross-section. The shoreline is located at X=40 km and the frontal zone starts near X= 60 km.

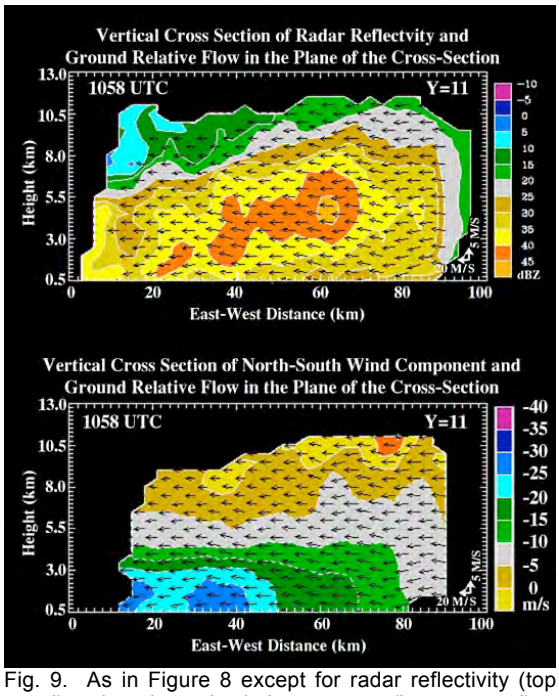

Fig. 9. As in Figure 8 except for radar reflectivity (top panel) and north-south wind component (bottom panel) at 1058 UTC.

With time, the strong flow and enhanced warm air advection associated with the land-falling hurricane moved the frontal zone westward towards land (Fig. 9). The gradients in wind speed across the frontal zone also decreased. A preliminary analysis suggests that the frontal zone propagation speed, about 28 m s^{-1}, was less than the speed at which the reflectivity features propagated (35 m s^{-1} from 75 degrees).

4.3 Deep Subsidence Zones

The horizontal and vertical cross-sections of radar reflectivity shown in figures 3, 7, 8, and 9 illustrate the variability of precipitation within the outer portions of Hurricane Isabel. Rather than consisting of a series of isolated spiraling convective bands, Isabel's outer rain bands were stratiform in character. But their internal structure often consisted of narrow gaps, or minima, in reflectivity between the more intense portions of the rainbands (c.f., X=30 to 40 km and X= 60 to 70 km in top panel of Fig. 8).

In general, the weak regions of radar reflectivity within the broader precipitation field coincided with regions of deep subsidence. At times, banded vertical velocity perturbations were oriented parallel to the curvature of the rain bands. This was most pronounced at mid-levels (Fig. 10). Peak magnitudes of vertical motion were typically <3 m s^{-1}.

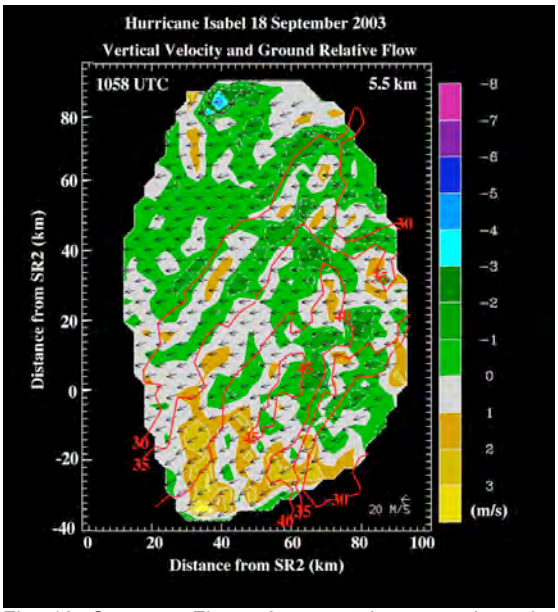

Fig. 10. Same as Figure 3, except here we show the vertical velocity at 5.5 km and 1058 UTC. Contours of radar reflectivity every 5 dB from 30 to 45 dBZ are overlaid for reference.

Regions of deep subsidence were implied in the statistical distribution of vertical drafts shown by Black et al. (1996) who examined vertical incidence Doppler data that are less susceptible to uncertainty in structure than the retrieved vertical drafts shown here.

The 12-minute period analyzed here suggests that these features may be continuous in time and could affect the distribution of precipitation through sublimation and evaporation in the downdraft branch and through vapor deposition and ice particle initiation in the updraft branch of the bands. It is interesting to note that the horizontal wavelength of the vertical velocity perturbation is about one-fourth the width of the broad stratiform rain band. It should be further noted that the broad rain band had multiple local maxima (c.f., Fig. 3) that may be a reflection of the banded vertical velocity perturbations.

5. CONCLUSIONS

A series of high temporal and spatial resolution analyses from a ground-based mobile dual-Doppler radar network revealed the complex structure of circulations associated with the outer bands of Hurricane Isabel during landfall along the North Carolina coast on 18 September 2003. A two-branch flow regime was observed with an easterly flow over the northern part of the domain and a northeasterly flow over the southern part of the domain. The northeasterly flow was associated with mean upward motion through a deep layer, extending below the melting level, while the easterly flow branch was associated with mean subsidence at nearly all levels. The high reflectivity portion of the rain band coincided with the northeasterly flow branch that contained a deep area-averaged updraft.

The distribution of land within the analysis domain suggests that the two-branch flow structure might be a result of interaction of the hurricane winds with the North Carolina coast. Regardless, strong convergence and turning of the wind was found to occur as the flow crossed the coastline. In the northern and southern extremes of the analysis domain, where the flow was oriented quasi-perpendicular to the coast, relatively shallow bands of convective drafts were observed. Peak vertical wind speeds in the convective drafts rarely exceed 5 m s^{-1}.

Zones of deep subsidence were diagnosed along the edges of the rain bands and in weak reflectivity regions between local maxima in the rain bands. These subsidence zones appeared to be part of a perturbation vertical velocity field that had banded structure oriented parallel to the curving rain bands at mid-levels. The temporal continuity and spatial scale of the vertical velocity bands suggested that they might be able to affect the distribution of precipitation.

In addition to the variation in circulations associated with flow over the land, a shallow frontal zone was observed just offshore. It was well marked by the change in height of the radar bright band that is indicative of melting at the 0° isotherm. A broad and sustained region of upward motion existed in the lowest 3 km of the atmosphere across the frontal zone and contributed to the area-averaged upward motion beneath the melting level in the northeasterly portion of the two-branch mesoscale circulation. In time, the frontal zone was pushed westward by the strong flow and warm air advection associated with the land-falling hurricane.

The detailed observations presented here illustrate the utility of mobile ground-based Doppler radars in studies related to land-falling tropical cyclones. Although not readily evident from the figures shown, careful inspection of the wind retrievals reveal that the 2 minute scanning strategy was more than sufficient to capture the evolution of the convective features in this hurricane. Individual features were easily traceable in time. Moreover, there was not an appreciable difference in the scale of resolvable features between the 2-minute and 4.5-minute volume scans.

This study represents the first time that convective-scale details of the four-dimensional flow over mesoscale regions have been obtained within a land-falling hurricane. It is hoped that the wind fields diagnosed here will be used to aid validation of numerical simulations of land-falling tropical cyclones in an effort to improve the forecasting of inland floods and damaging winds.

6. ACKNOWLEDGMENTS

Support for R. Curry was provided by the National Science Foundation Research Experience for Undergraduates Program through grant EEC-0313747. The Isabel SMART radar deployment was funded by NASA under grant NAG5-13262 and through the Cooperative Institute for Mesoscale Meteorological Studies at the University of Oklahoma. Dr. J. Schroeder and students

from Texas Tech University were instrumental in the data collection. G. Carrie contributed valuable insight, software support, and leadership throughout the project.

7. REFERENCES

Barnes, G.M., E. J. Zipser, D. Jorgenson, and F. Marks, 1983: Mesoscale and Convective Structure of a Hurricane Rainband. *J. Atmo. Sci.*, **40**, 2125–2137.

Barnes, G. M., J. F. Gamache, M. A. LeMone, and G. J. Stossmeister, 1991: A convective cell in a hurricane rainband. *Mon. Wea. Rev.*, **119**, 776-794.

Beven, J. and H. Cobb. Cyclone Report: Hurricane Isabel. National Hurricane Center. Available http://www.nhc.noaa.gov/2003isabel.shtml.

Biggerstaff, M. I. and R. A. Houze, Jr., 1991: Kinematic and precipitation structure of the 10-11 June 1985 squall line. *Mon. Wea. Rev.,* **119**, 3034-3065,

Biggerstaff, M. I., L. J. Wicker, J. Guynes, C. Ziegler, J. M. Straka, E.N. Rasmussen, A. Dogget IV, L. D. Carey, J. L. Schroeder, and C. Weiss, 2005: The Shared Mobile Atmospheric Research and Teaching (SMART) Radar: A collaboration to enhance research and teaching. *Bull. Amer. Meteor. Soc.*, **86**, 1263-1274.

Black, R. A., H. B. Bluestein, and M. L. Black, 1994: Unusually strong vertical motions in a Caribbean hurricane. *Mon. Wea. Rev.*, **122**, 2722-2739.

Black, M. L., R. W. Burpee, and F. D. Marks, Jr., 1996: Vertical motion characteristics of tropical cyclones determined with airborne Doppler radial velocities. J. Atmos. Sci., 53, 1887-1909.

Elsberry, Russell L., 2002: Predicting hurricane landfall precipitation. *Bull. Amer. Meteor. Soc., **83,*** 1333-1339.

Gentry, R. C., 1983: Genesis of tornadoes associated with hurricanes. *Mon. Wea. Rev.,* **111,** 1793–1805.

Jones, R. W., 1987: A simulation of hurricane landfall with a numerical model featuring latent heating by the resolvable scales. Mon. Wea. Rev., **115**, 2279-2297.

Jorgensen, D. P., 1984: Mesoscale and convective-scale characteristics of mature hurricanes. Part I: General observations by research aircraft. *J. Atmos. Sci.*, **41**, 1268-1285.

Jorgensen, D. P., E. J. Zipser, and M. A. LeMone, 1985: Vertical motions in intense hurricanes. *J. Atmos. Sci.*, **42**. 839-856.

Leise, J.A., 1981: A multi-dimensional scale-telescoped filter and data extension package. NOAA Technical Memo, WPL-82, 20pp.

Marks, F. D., and R. A. Houze, Jr., 1987: Inner Core Structure of Hurricane Alicia from Airborne Doppler Radar Observations. *J. Atmo. Sci.*, **44,** 1296–1317.

Marks, F. D., L. K. Shay, and others, 1998: Landalling tropical cyclones: Forecast problems and research opportunities. *Bull. Amer. Meteor. Soc.*, **79**, 305-323.

McCaul, E. W., Jr., Jr., 1987: Observations of the Hurricane ‘‘Danny’’ tornado outbreak of 16 August 1985. *Mon. Wea. Rev.,* **115,** 1206–1223.

Mohr, C., L. Miller, R. Vaughan, and H. Frank, 1986: The merger of mesoscale datasets into a common Cartesian format for efficient and systematic analyses. *J. Atmos. and Oceanic Technol.,* **3,** 143-161.

Oye, R., C. Miller, and S. Smith, 1995: Software for Radar Visualization, Editing, and Interpolation. *Preprints, 27th Conference on Radar Meteorology.* Vail, CO. Amer. Meteor. Soc., 359-361.

Rappaport, E. N., 2000: Loss of life in the United States associated with recent Atlantic tropical cyclones. *Bull. Amer. Meteor. Soc.*, **81**, 2065-2073.

Wurman, J., J. Straka, E. Rasmussen, M. Randall, and A. Zahrai, 1997: Design and Deployment of a Portable, Pencil-Beam, Pulsed, 3-cm Doppler Radar. *J. Atmos. and Oceanic Tech.,* **14**, 1502–1512.